Brain Acetylcholinesterase Activity: Validation of a PET Tracer in a Rat Model of Alzheimer's Disease

Toshiaki Irie, Kiyoshi Fukushi, Hiroki Namba, Masaomi Iyo, Hiroshi Tamagami, Shin-ichiro Nagatsuka and Nobuo Ikota

Division of Clinical Research and Division of Chemical Pharmacology, National Institute of Radiological Sciences; Division of Neurosurgery, Chiba Cancer Center Hospital; National Institute of Mental Health, National Center of Neurology and Psychiatry, Chiba; and Tokai Research Laboratories, Daiichi Pure Chemicals Co., Ibaragi, Japan

We developed three radioactive acetylcholine analogs—N[^{14}C]methyl-4-piperidyl acetate ([^{14}C]MP4A), propionate ([^{14}C]MP4P) and isobutyrate ([^{14}C]MP4IB)—as radiotracers for measuring brain acetylcholinesterase (AchE) activity in vivo. The principle of our method is that the lipophilic analog diffuses into the brain where it is metabolized by AchE to produce a hydrophilic metabolite, which is trapped at the site of its production. The purpose of this study was to examine whether the tracers would have the sensitivity needed for early diagnosis of Alzheimer's disease using rats with a unilateral lesion in the nucleus basalis magnocellularis (NBM), an animal model of the cholinergic deficit in Alzheimer's disease. **Methods:** Rats with a unilateral NBM lesion were prepared, and the N[^{14}C]methyl-4-piperidyl esters and N-Isopropyl-*p*-[^{123}I]iodoamphetamine ([^{123}I]IMP) were injected intravenously 30 and 2 min, respectively, before the rats were killed. Uptake of ^{14}C and ^{123}I and AchE activity in the lesioned and unlesioned (control) sides of the cortex were measured simultaneously. **Results:** The NBM lesion showed reduced cortical AchE activity by 30%–50%, with no side-to-side differences in [^{123}I]IMP uptake. Autoradiographic studies showed that uptake of ^{14}C from [^{14}C]MP4A and [^{14}C]MP4P was significantly lower in the lesioned than unlesioned side of the cortex, which agreed well with the AchE histochemical staining patterns. Tissue dissection studies showed different uptake changes for the three compounds when AchE activity in the lesioned side of the cortex was reduced by 50%: ^{14}C uptake from [^{14}C]MP4P, [^{14}C]MP4A and [^{14}C]MP4IB was reduced by 27%, 21% and 7.3%, respectively. Theoretical analysis of the observed sensitivities of the tracers in relation to their in vitro enzymatic properties indicated that tracer sensitivity was highly dependent on the enzymatic hydrolysis rate of the tracer. **Conclusion:** The [^{14}C]MP4A and [^{14}C]MP4P esters had sufficient sensitivity to enable AchE activity changes in the rat cortex of less than 50% to be detected, indicating that the present method is applicable to PET diagnosis of Alzheimer's disease.

Key Words: acetylcholinesterase; Alzheimer's disease; PET; biochemical validation study

J Nucl Med 1996; 37:649–655

Since the initial report by Pope et al. (*1*) in 1965, the degeneration of brain cholinergic systems has proved to be the most consistent neurochemical deficit in patients with Alzheimer's disease (*2–4*), although other, noncholinergic changes are also observed in the brain of such patients (*5*). A number of cholinergic radioligands, such as [^{123}I]IQNB (*6,7*), [^{11}C]NMPB (*8*), [^{11}C]dexitimide (*9*), [^{11}C]benztropine (*10*), [^{11}C]scopolamine (*11*) and [^{123}I]IBVM (*12–15*), have been developed and used for the evaluation of central cholinergic systems using PET and SPECT. Postmortem studies in patients with Alzheimer's disease indicated that among cholinergic biochemical markers, the most profound change, compared with normal subjects, is a reduction in the activity of two acetylcholine-related enzymes—choline acetyltransferase and acetylcholinesterase (AchE)—in the neocortex and hippocampus. These enzymes are attractive target molecules for the design of tracers to detect cholinergic changes in Alzheimer's disease. Some attempts to do this using various radiolabeled inhibitors of AchE, such as [^{11}C]sarin (*16*), [^{11}C]physostigmine (*17,18*) and others (*19,20*) have been reported.

Another method of mapping brain AchE using PET may be to design a radiotracer of the metabolic trapping type. As examples of such a tracer, we synthesized d,l-N[^{14}C]methyl-3-piperidyl acetate and its congeners with longer acyl groups ([^{14}C]MP3X series) and N[^{14}C]methyl-4-piperidyl acetate and its congeners ([^{14}C]MP4X series) according to the biochemical rationale shown in Figure 1. Briefly, the principle of our method is that a lipophilic acetylcholine analog enters the brain readily through the blood–brain barrier and is hydrolyzed by AchE to produce a hydrophilic product, to which the barrier has limited permeability, that essentially becomes trapped in the brain at the site of the hydrolytic enzyme. In our previous studies, some acetylcholine analogs showed high specificity for mouse brain AchE, and treating mice with them resulted in long-term retention of radioactivity in the brain (*21*). We also visualized brain AchE activity in rats and a monkey by autoradiography and PET using d,l-N[^{11}C/^{14}C]methyl-3-piperidyl acetate as a tracer (*22*).

The aim of the present study was to assess the applicability of the radioactive analog method for measuring the reduction in cortical AchE activity that occurs in patients with Alzheimer's disease using PET. To determine whether acetylcholine analog tracers of the MP4X series would have the sensitivity needed to detect changes in cortical AchE activity corresponding to the early stages of Alzheimer's disease, we used rats with reduced cortical AchE activity induced by a lesion in the nucleus basalis magnocellularis (NBM). The relationships between the experimentally measured changes in tracer uptake and AchE activity are explained on the basis of a three-compartment model and the enzymatic properties of the tracers, determined in vitro. The applicability of the radioactive acetylcholine analog method for PET studies in patients with Alzheimer's disease is also discussed.

MATERIALS AND METHODS

Radiotracers and Chemicals

Carbon-14-methyl-4-piperidyl acetate ([^{14}C]MP4A), propionate ([^{14}C]MP4P), isobutyrate ([^{14}C]MP4IB) and N[^{14}C]methyl-4-piperidinol ([^{14}C]MP4OH) were prepared by reacting their demethyl compounds with [^{14}C]methyl iodide (2.0–2.1 GBq/mmole), as reported previously (*21*). The radiochemical purities of the labeled compounds after formulation for animal studies were greater than 95%. N-Isopropyl-*p*-[^{123}I]iodoamphetamine ([^{123}I]IMP, 74 MBq/μmole); and 1,5-bis(4-allyldimethyl-ammoniumphenyl)-pentan-3-one dibromide (AchE inhibitor, BW284c51) were obtained commercially.

Received Feb. 6, 1995; revision accepted June 7, 1995.

For correspondence or reprints contact: Toshiaki Irie, PhD, Division of Clinical Research, National Institute of Radiological Sciences 9-1, Anagawa-4-chome, Inage-ku, Chiba-shi 263, Japan.

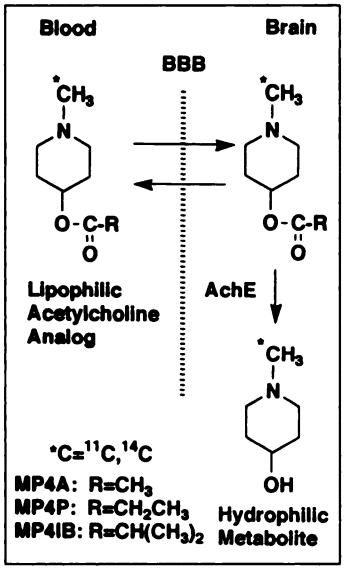

FIGURE 1. Schematic diagram representing the biochemical rationale of the radioactive acetylcholine analog method for measuring AchE activity in the brain by PET and autoradiography. BBB = blood–brain barrier.

All other chemicals used were of the highest grade available commercially.

Radioactivity Measurement by an Imaging Phosphor Plate

The ^{14}C radioactivity on thin-layer chromatographic (TLC) plates and the ^{14}C and ^{123}I radioactivities in the tissue sections used for autoradiography were quantitated using an imaging phosphor plate and an image analysis system. Compared with conventional x-ray film methods, the imaging phosphor plate method has the advantages of a wide dynamic range, high sensitivity, linearity of response and digitized output, which make it particularly useful for quantitative analysis of ^{14}C and ^{123}I in double-nuclide autoradiography.

In Vitro Characterization of Tracer Properties

Octanol–Water Partition Coefficient. The required N[^{14}C]methyl-4-piperidyl ester ([^{14}C]MP4A, [^{14}C]MP4P or [^{14}C]MP4IB) or [^{14}C]MP4OH was added to a 1:1 mixture of 1-octanol and 10 m*M* phosphate buffer (pH 7.4), shaken vigorously and allowed to equilibrate for 1 hr at room temperature. The ^{14}C concentrations in the organic and aqueous phases were measured with a liquid scintillation counter, and each partition coefficient was calculated as the ratio of the concentration in the organic phase to that in the aqueous phase.

Enzymatic Hydrolysis Rate. Cerebral cortical tissues were obtained from three male Wistar rats (280–330 g, 9-wk-old), weighed and homogenized in 10 vol ice-cold 0.1 *M* phosphate buffer, pH 7.4, with a glass–Teflon homogenizer. Each homogenate (200 μl) was preincubated for 5 min at 37°C. The required N[^{14}C]methyl-4-piperidyl ester (74 kBq, 20 μl) was added and incubated at 37°C with gentle shaking for the appropriate time, after which a 50-μl 2 *N* HCl solution was added to terminate the reaction, and the mixture was immersed in an ice bath. Next, 5 μl of reaction mixture was applied to a silica-gel TLC plate and developed with ethyl acetate–isopropanol–ammonia (15:5:1 v/v/v). The TLC plate was air-dried, exposed to HCl vapor to fix the ^{14}C radioactivity, wrapped with covering foil (5 μm thick) and placed in a cassette in contact with the imaging phosphor plate for 1 hr. The radioactivities corresponding to the unchanged ester (Rf values: [^{14}C]MP4A = 0.74; [^{14}C]MP4P = 0.77; [^{14}C]MP4IB = 0.77) and the hydrolysis product (Rf value: [^{14}C]MP4OH = 0.41) were quantitated using the BAS 2000 system. The enzymatic hydrolysis rate (K) of each tracer was calculated as follows:

$$K = \frac{\ln A_1 - A_2}{(T_2 - T_1) \cdot C}$$

where A_1 and A_2 represent the ^{14}C radioactivity of the unchanged ester remaining at times T_1 and T_2, respectively; and C represents the brain tissue concentration (in grams per milliliter) in the reaction solution.

Acetylcholinesterase Specificity. It has been reported that BW284c51 (30 μ*M*) inhibits AchE completely and selectively (*23,24*). To determine the AchE specificities of the N[^{14}C]methyl-4-piperidyl esters in the rat cerebral cortex, BW284c51 (0.36 m*M*, 20 μl) was added to the cortical tissue homogenates (200 μl) and preincubated for 5 min at 37°C, after which the hydrolysis rate (K′) in the presence of this inhibitor was measured, as described before. The specificity (S) of each N[^{14}C]methyl-4-piperidyl ester for AchE was calculated as follows:

$$S\ (\%) = 100 \times (K - K')/K,$$

where K′ and K are the first-order rate constants for hydrolysis by the homogenate with and without the AchE inhibitor, respectively.

Measurement of Regional Cerebral Blood Flow and AchE Activity

The relative blood flow in brain regions was measured using [^{123}I]IMP. The rats were intravenously injected (i.v.) with [^{123}I]IMP and killed 2 min later (*25*). The brain tissues were dissected out and weighed, and the ^{123}I radioactivity was measured. The AchE activity in rat brain was measured by the method of Ellman et al. (*26*) using brain tissue homogenates diluted with 0.1 *M* phosphate buffer, pH 7.4, at room temperature.

Brain Regional Kinetics of Carbon-14 MP4P and Carbon-14 MP4OH in Normal Rats

Normal rats were injected i.v. with [^{14}C]MP4P or [^{14}C]MP4OH (both 370 kBq/0.3 ml; n = 15 per compound), and three rats were killed 1, 5, 15, 30 and 60 min after injection. The striatum, cerebral cortex and cerebellum were dissected out and weighed, and the ^{14}C radioactivity in each was measured.

Chemical Form Analysis of Carbon-14 Radioactivity in Brain

Three rats were injected with [^{14}C]MP4P and killed 5 min after injection, and the brain tissues were frozen rapidly by immersion in an acetone–dry-ice bath. About 50 mg of each frozen tissue was homogenized in methanol–phosphate buffer (1:1 v/v) in the presence of BW284c51 (30 μ*M*). The radioactivity of the radioactive metabolite [^{14}C]MP4OH in the homogenate was determined by the TLC method described before and expressed as a percentage of the total radioactivity in the homogenate.

Simultaneous Measurement of Tracer Uptake, Blood Flow and AchE Activity in Unilateral NBM-Lesioned Rats

Dissection Method. The NBM-lesioned rats were prepared as follows. Rats (280–330 g) were anesthetized with 50 mg/kg pentobarbital administered intraperitoneally and placed in a stereotaxic instrument; 10 μg ibotenic acid in 1 μl 0.1 *M* phosphate-buffered saline, pH 7.4, was infused into the left NBM for 10 min at a flow rate of 0.1 μl/min (*27*). Two weeks after surgery, the rats (n = 5 per compound) were injected i.v. with the required ^{14}C-labeled ester (370 kBq/0.3 ml) and [^{123}I]IMP (1.1 MBq/0.3 ml) 30 and 2 min, respectively, before they were killed. Both sides of the neocortex were removed, weighed and homogenized, as described before. Each homogenate was diluted with 0.1 *M* phosphate buffer, pH 7.4, as appropriate, and the AchE activity was measured. Another portion of the same diluted homogenate was used to measure the ^{123}I radioactivity with a gamma counter and that of ^{14}C with a liquid scintillation counter after the ^{123}I had decayed. The uptake of radioactivity from each ester was expressed as the percent dose per gram of wet tissue.

TABLE 1
Hydrolysis Rate and AchE Specificity of Carbon-14-Methyl-4-Piperidyl Esters in Rat Cortical Homogenate

Compound	Hydrolysis rate in homogenate (fraction/min/g/ml, 37°C)* Without inhibitor (A) (mean ± s.d.)	With inhibitor (B)† (mean ± s.d.)	AchE specificity (%) (A − B)A
[^{14}C]MP4A	2.32 ± 0.39	0.050 ± 0.004	98
[^{14}C]MP4P	0.62 ± 0.09	0.076 ± 0.017	88
[^{14}C]MP4IB	0.108 ± 0.008	0.055 ± 0.003	49

*First-order rate constant at tissue concentration of 1 g/ml.
†BW284c51 (30 μM) was used as a specific inhibitor of AchE.

Autoradiographic Method. The NBM-lesioned rats were injected intravenously with [^{14}C]MP4A or [^{14}C]MP4P (370 kBq/0.3 ml) and [^{123}I]IMP (3.7 MBq/0.3 ml) 30 and 2 min, respectively, before sacrifice. The brain tissues were removed and frozen in a freezer at −80°C for 30 min, and the frozen tissues were cut into 20-μm-thick coronal sections. Each section was thawed on a cover glass, exposed to HCl vapor, dried on a hotplate for 5 min at 50°C and placed in a cassette in contact with an imaging phosphor plate for 1–2 hr to record the ^{123}I radioactivity by the BAS 2000 system. Two weeks later, when the ^{123}I had decayed completely, the ^{14}C activity was recorded using another imaging phosphor plate. Under these conditions, the crosstalk of the ^{14}C to the ^{123}I image was less than 4%. For AchE histochemical study, a section adjacent to that used for autoradiography was mounted on a slide-glass, and the AchE activity was stained histochemically using a routine method (*28*).

RESULTS

The biochemical properties of the three N[^{14}C]methyl-4-piperidyl esters ([^{14}C]MP4A, [^{14}C]MP4P and [^{14}C]MP4IB) were characterized in rat brain tissue homogenates in vitro. All esters were stable in 0.1 *M* phosphate buffer, pH 7.4, at 37°C with first-order rate constants of nonenzymatic hydrolysis of less than 5×10^{-5} fraction/min but were hydrolyzed rapidly to produce [^{14}C]MP4OH when incubated with rat cortical homogenates (Table 1). The highest hydrolysis rate (2.32 fraction/min at 37°C) was observed with [^{14}C]MP4A, which is an analog of acetylcholine with the same acyl group, at a tissue concentration of 1 g/ml. The esters with larger acyl moieties were hydrolyzed more slowly: the relative hydrolysis rates of [^{14}C]MP4A, [^{14}C]MP4P and [^{14}C]MP4IB were 1.0, 0.27 and 0.05, respectively. To determine the specificity of each tracer for AchE in the brain, we performed an inhibition study. When 30 μM BW284c51, a specific inhibitor of AchE, was added to the cortical homogenates, the hydrolysis rates of the three esters were reduced considerably and became almost identical. From the differences between the rates with and without the inhibitor, the rat cortical specificities of [^{14}C]MP4A, [^{14}C]MP4P and [^{14}C]MP4IB for AchE were estimated to be 98%, 89% and 49%, respectively.

The physicochemical properties and brain regional kinetics of the tracers were examined. The time course of ^{14}C uptake in three brain regions (striatum, cortex and cerebellum) of normal rats after i.v. injection of [^{14}C]MP4P and [^{14}C]MP4OH is shown in Figure 2. The initial uptake of [^{14}C]MP4P in each brain region was much higher than that of [^{14}C]MP4OH. These results are compatible with their lipophilicities measured in vitro: the octanol/water partition coefficients of [^{14}C]MP4P and [^{14}C]MP4OH were 0.5 and 0.008, respectively. The brain uptake of the hydrophilic metabolite ([^{14}C]MP4OH) remained

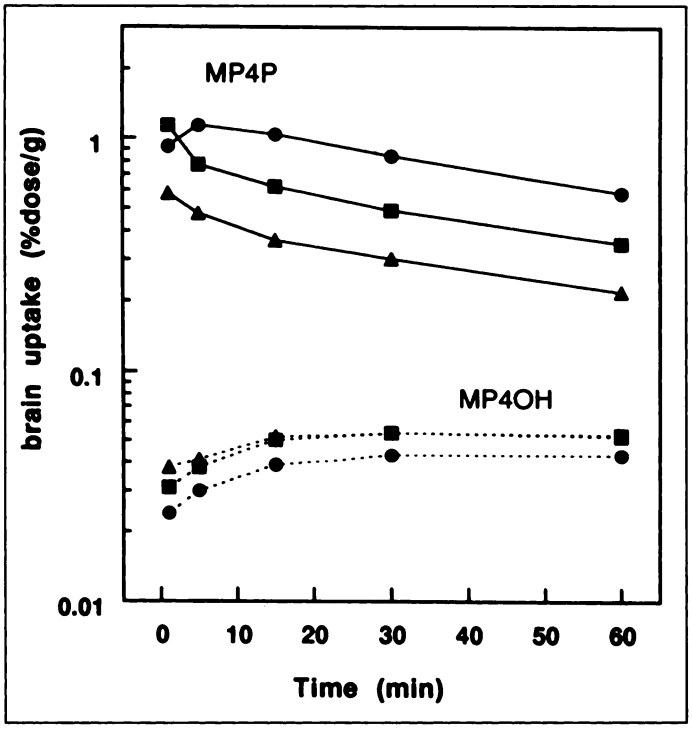

FIGURE 2. Comparison of brain kinetics curves between the lipophilic ester [^{14}C]MP4P and the hydrophilic metabolite [^{14}C]MP4OH after intravenous administration in normal rat. Data are shown as mean values with s.d. for three rats per time point: striatum (●), cerebral cortex (■) and cerebellum (▲).

low, indicating that the permeability of the blood–brain barrier to this metabolite is limited. In the case of the propionate ester ([^{14}C]MP4P), after an initial high incorporation rate, the ^{14}C radioactivity elimination from the three brain regions followed monoexponential curves with the same elimination rate, with half-lives of approximately 60 min. The rank order of ^{14}C uptake from [^{14}C]MP4P by the three brain regions during the stationary phase (15–60 min after injection) agreed with that of the AchE activity: Striatum > Cortex > Cerebellum. Chemical form analysis of the ^{14}C radioactivity in the brain revealed that more than 99% of the ^{14}C radioactivity in the cortex was in the form of the radioactive metabolite [^{14}C]MP4OH 5 min after i.v. injection of [^{14}C]MP4P. Because the uptake ratios of these three brain regions were constant 15–60 min after injection, the 30-min postinjection uptake values were used in the following experiments.

Fifteen rats with a unilateral NBM lesion (n = 5 per compound) were given the required N[^{14}C]methyl-4-piperidyl ester and [^{123}I]IMP (for assessment of cerebral blood flow) 30 and 2 min, respectively, before sacrifice. Uptake of ^{14}C and ^{123}I radioactivity and AchE activity in both sides of the cerebral cortex were measured simultaneously in each rat. No side-to-side blood flow differences were observed: uptake of ^{123}I in the lesioned side was 98.5% ± 2.3% (n = 15, mean ± s.d.) of that in the control side. The NBM lesion reduced cortical AchE activity in the ipsilateral side by 30%–50%, with some inter-animal variation (Table 2). Both [^{14}C]MP4A and [^{14}C]MP4P, which had high AchE specificity (Table 1), reduced ^{14}C uptake in the lesioned side significantly: [^{14}C]MP4A reduced ^{14}C uptake by an average of 19% compared with a reduction in AchE activity of 45%; the respective values for [^{14}C]MP4P were 27% and 50%. In contrast, [^{14}C]MP4IB, which had a relatively low specificity for AchE (49%), evoked a much smaller response: the average reduction in ^{14}C uptake was 3% compared with 29% for AchE activity. The rank order of ^{14}C

TABLE 2
Reduction of AchE Activity and Carbon-14 Uptake Simultaneously Measured in Rats with Unilateral NMB Lesion

Compound/Rat no.	AchE activity* Control side	AchE activity* Lesioned side	AchE activity* % Reduction	^{14}C uptake† Control side	^{14}C uptake† Lesion side	^{14}C uptake† % Reduction
[^{14}C]MP4A						
1	4.15	2.68	−35	0.570	0.493	−14
2	4.13	2.53	−39	0.621	0.527	−15
3	3.98	2.12	−47	0.538	0.431	−20
4	3.99	1.99	−50	0.528	0.436	−17
5	3.96	1.86	−53	0.636	0.462	−27
			−45 (avg.)			−19 (avg.)
[^{14}C]MP4P						
1	3.70	2.06	−44	0.483	0.376	−22
2	3.81	2.10	−45	0.494	0.370	−25
3	3.60	1.81	−50	0.474	0.347	−27
4	3.56	1.76	−50	0.478	0.361	−25
5	4.03	1.54	−62	0.519	0.333	−36
			−50 (avg.)			−27 (avg.)
[^{14}C]MP4IB						
1	3.56	2.73	−23	0.192	0.185	−4
2	3.28	2.47	−25	0.191	0.181	−5
3	3.33	2.49	−25	0.203	0.200	−1
4	3.29	2.26	−31	0.191	0.193	1
5	3.19	1.92	−40	0.176	0.165	−6
			−29 (avg.)			−3 (avg.)

*nmole/mg of tissue/min.
†%dose/g of tissue 30 min after injection.
avg. = average.

uptake reduction correlated with that of AchE activity reduction for both [^{14}C]MP4A and [^{14}C]MP4P (Kendall rank correlation: MP4A, $p = 0.05$; MP4P, $p = 0.14$).

Because the average reduction in AchE activity differed among the three compounds, we corrected for this difference to obtain the normalized sensitivity for each compound for detection of changes in AchE activity. On the basis of the results presented in Table 2, we extrapolated the percent ^{14}C uptake reduction under the conditions of a 50% reduction in AchE activity in the lesioned side, termed R_{50} (^{14}C uptake reduction at 50% AchE activity reduction). The R_{50} values for [^{14}C]MP4P, [^{14}C]MP4A and [^{14}C]MP4IB ($n = 4$ for [^{14}C]MP4IB; data for rat no. 4 were omitted because ^{14}C uptake increased in the lesioned side) were 27%, 21% and 7.3%, respectively.

The autoradiograms of the same coronal sections 30 min after injection of [^{14}C]MP4A and [^{14}C]MP4P and 2 min after [^{123}I]IMP and the AchE histochemical staining of the adjacent sections are shown in Figure 3. The [^{123}I]IMP images demonstrated no side-to-side blood flow differences, particularly in the cortex. In contrast, the lesioned (left) side of the cortex showed obvious reductions in ^{14}C uptake and AchE activity compared

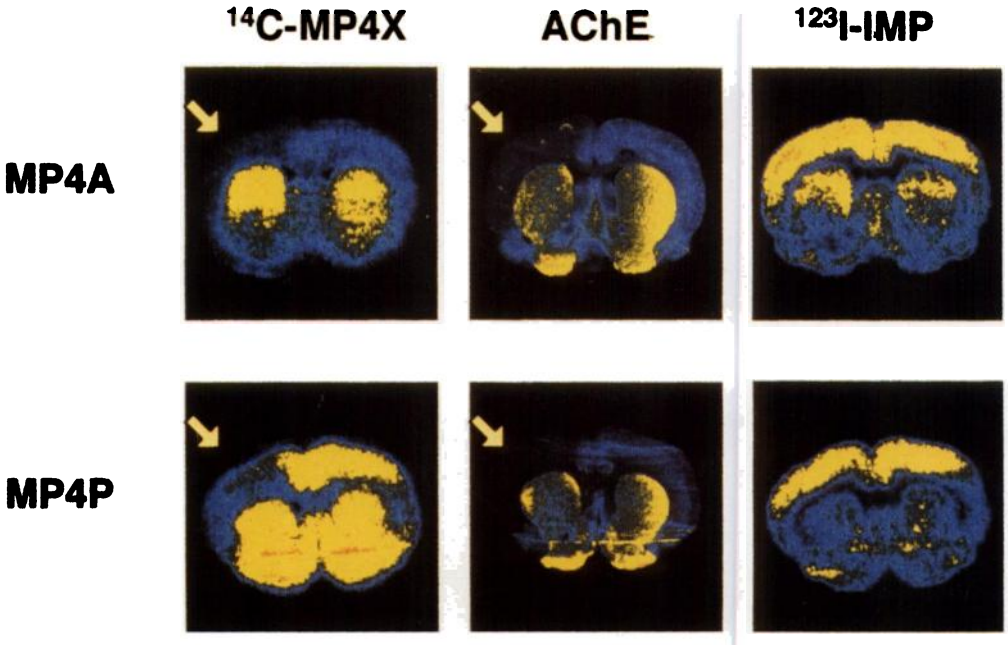

FIGURE 3. Brain autoradiograms of [^{14}C]MP4A and [^{14}C]MP4P, histochemical AchE studies and blood flow images measured by [^{123}I]IMP in rats with a unilateral lesion of the NBM. Decreases in ^{14}C radioactivity, superimposed on diminished histochemical staining of AchE, are observed in cerebral cortices on the lesioned side (arrowhead), with no side-to-side difference in blood flow.

TABLE 3
Percent Reduction of Carbon-14 Uptake at 50% AchE Change: Calculated and Observed Values

Compound	Control side of cortex			Lesioned side of cortex			% Reduction of ^{14}C Uptake	
	$k_{AchE} \times$ [AchE]	$k_{Others} \times$ [Others]	RF(c)	$k_{AchE} \times$ [AchE]	$k_{Others} \times$ [Others]	RF(l)	Calculated R_{50}	Observed R_{50}
[^{14}C]MP4A	2.274	0.046	0.570	1.137	0.046	0.403	29	21
[^{14}C]MP4P	0.546	0.074	0.262	0.273	0.074	0.165	37	27
[^{14}C]MP4IB	0.053	0.055	0.058	0.026	0.055	0.044	24	7

with the unlesioned side: the distribution of ^{14}C radioactivity in each lesioned side was superimposed exactly on the staining pattern of AchE activity, which decreased in the cortical region, sparing the cingulate and entorhinal cortices.

DISCUSSION

Extensive reduction of AchE activity is known to occur in the neocortex and hippocampus of patients with Alzheimer's disease (*1,4*), and its extent correlates with the senile plaque count and disease severity (*3*). To measure brain AchE activity by PET, we designed several radioactive acetylcholine analogs (d,l-N[^{14}C]methyl-3-piperidyl esters [MP3X series] and N[^{14}C]methyl-4-piperidyl esters [MP4X series]). In our previous study of mice, some of these analogs (e.g., d,l[^{14}C]MP3A and [^{14}C]MP4A) (*21*) had high AchE specificity and resulted in long-term retention of radioactivity in the brain. We also demonstrated that [^{11}C/^{14}C]-d,l-MP3A can be used to visualize brain AchE activity in the monkey by PET and in NBM-lesioned rats by autoradiography (*22*). In the present study, we assessed the sensitivities of tracers of the MP4X type, which have no optical isomers, in unilateral NBM-lesioned rats and examined the dependency of their sensitivities on their physical and enzymatic properties.

To validate the sensitivity of a tracer, the true value of the biochemical change in question must be established in animal experiments. In the present study, we used rats with a unilateral NBM lesion, an animal model of the cholinergic deficit in Alzheimer's disease (*29*). The rat NBM is homologous to the nucleus of Meynert in humans and provides a major cholinergic innervation to the neocortex. It is known that a unilateral NBM lesion results in selective reduction of cortical cholinergic markers, such as choline acetyltransferase and AchE, in the lesioned side without affecting markers of other transmitter systems (*30*) or cortical blood flow (*27,31*). These properties of the model help to clarify the relationship between the uptake of [^{14}C]MP4X and AchE activity in the brain because [^{14}C]MP4X is highly lipophilic, and its uptake into brain tissues is dependent on blood flow. In the autoradiographic study (Fig. 3), the feasibility of using unilateral NBM-lesioned rats to validate the tracers was demonstrated: ^{14}C uptake from both [^{14}C]MP4A and [^{14}C]MP4P in the neocortex of the lesioned side was reduced significantly and corresponded to the reduced AchE activity, which was detected histochemically, without any side-to-side differences in [^{123}I]IMP uptake.

In the tissue dissection study in NBM-lesioned rats (Table 2), we measured the lesion/control ratios of uptake from three N[^{14}C]methyl-4-piperidyl esters ([^{14}C]MP4A, [^{14}C]MP4P and [^{14}C]MP4IB) directly, the relative blood flow tracer ([^{123}I]IMP) uptake and the AchE activity. The lack of side-to-side cortical blood flow differences was confirmed in 15 rats with a unilateral NBM lesion (lesion-to-control ratio: 98.5% ± 2.3%). Rats given [^{14}C]MP4A and [^{14}C]MP4P showed significantly reduced ^{14}C uptake in the lesioned side compared with the control side, whereas the uptake reduction after [^{14}C]MP4IB was much lower, as was the change in AchE activity (29% reduction), than that after [^{14}C]MP4A (45%) and [^{14}C]MP4P (50%). Because changes in AchE activity varied among the groups, we introduced R_{50} values (see Results and observed R_{50} values in Table 3) to evaluate the sensitivity of the tracers for a reduction in AchE activity of 50%. The order of relative sensitivity was [^{14}C]MP4P > [^{14}C]MP4A > [^{14}C]MP4IB, as for the autoradiography study, where ^{14}C uptake for [^{14}C]MP4P showed higher contrast than that for [^{14}C]MP4A.

As discussed by Kilbourn (*32*), to validate a radiotracer, the relevant disease and sensitivity required must be identified. The AchE activity in the neocortex of patients with Alzheimer's disease has been reported to be reduced by 50%–90% compared with that in age-matched control subjects (*4*). Therefore, for a differential diagnosis in patients with and without Alzheimer's disease, tracers sensitive enough to detect a 50% reduction in cortical AchE activity are considered clinically useful. The observed R_{50} values of [^{14}C]MP4A (21%) and [^{14}C]MP4P (27%) indicated that both are sufficiently sensitive to detect a 50% reduction in cortical AchE activity in rats—the extent of AchE reduction corresponding to a differential diagnosis of Alzheimer's disease. Furthermore, in patients with a low plaque count, corresponding to the early stages of Alzheimer pathology, a linear correlation between AchE activity and plaque count has been reported (*3*). The observed R_{50} values of [^{14}C]MP4A (21%) and [^{14}C]MP4P (27%) and the correlation between their rank order of ^{14}C uptake and AchE activity reduction suggest that both tracers may enable the detection of a reduction of less than 50% in cortical AchE activity, resulting an even earlier diagnosis of Alzheimer's disease.

As discussed before, with the present method, the three esters with different enzymatic properties showed different R_{50} values (i.e., the sensitivity of these tracers to detect a 50% reduction in AchE activity differed). We considered the relationship between the tracer's sensitivity and its enzymatic properties (specificity for and reactivity with AchE) on the basis of the three-compartmental model shown in Figure 4. This model is the same as that of Lassen et al. (*33*) for ^{99m}Tc-HMPAO and

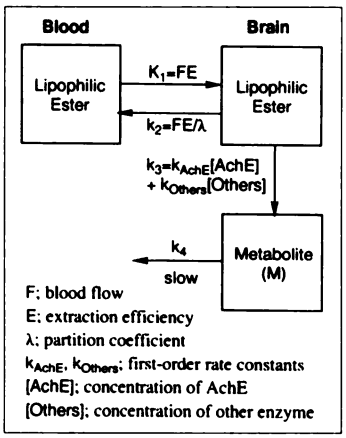

FIGURE 4. Three-compartment model describing the kinetic behavior of N[^{14}C]methyl-4-piperidyl esters in the brain.

describes the kinetic behavior of [^{14}C]MP4X in the brain. From the model (Appendix, Equation A2), we can predict that the tracer uptake (M) or, more correctly, the retention fraction (RF) will depend in a nonlinear manner on the metabolic rate of the tracer in the target region, k_{AchE}[AchE]: when the metabolic rate is much higher than the elimination rate (FE/λ), RF approaches unity. In this situation, uptake becomes independent of AchE activity. However, when the metabolic rate is low, RF becomes dependent on AchE activity in a directly proportional manner.

In the second part of the Appendix, the method of calculating the theoretical R_{50} value (calculated R_{50}, Table 3) is described on the basis of the tracers' enzymatic properties determined in vitro (Table 1) and Equations A3–A5 derived from the model. The calculated R_{50} values for [^{14}C]MP4A and [^{14}C]MP4P agreed with the observed R_{50} values in NBM-lesioned rats (Table 3). The order of the R_{50} values of [^{14}C]MP4A and [^{14}C]MP4P ([^{14}C]MP4P > [^{14}C]MP4A) indicates that [^{14}C]MP4P has a higher sensitivity than [^{14}C]MP4A, which was due not to tracer specificity for AchE ([^{14}C]MP4A [98%] > [^{14}C]MP4P [88%]) (Table 1), but to tracer reactivity with AchE (AchE reactivity: [^{14}C]MP4P, 0.62 fraction/min; [^{14}C]MP4A, 2.32 fraction/min) (Table 1): the lower the reactivity, the higher the sensitivity. However, the calculated R_{50} value for [^{14}C]MP4IB (24%) differed considerably from the observed R_{50} value (7%), which suggests that the sensitivity of [^{14}C]MP4IB observed in NBM-lesioned rats was much lower than that expected from its enzymatic properties. The low observed R_{50} value of [^{14}C]MP4IB can be attributed, in part, to its low brain uptake (0.19% dose/g) and the noise from the blood-borne radioactive metabolite: the radioactive metabolite formed in peripheral tissues entered the brain slowly (0.05% dose/g 30 min after injection of [^{14}C]MP4OH), which may have reduced the differential ^{14}C uptake in the two sides of the cortex (if the reactivity is too low, the sensitivity is also low). Therefore, with the present method, suitable adjustment of tracer reactivity with AchE is needed to enable changes in AchE activity in the target region to be detected with high sensitivity and accuracy.

Nonlinearity of tracer response is also shown in Figure 2: The striatum-to-cortex ratio of ^{14}C uptake 30 min after administration of [^{14}C]MP4P was 1.8, whereas that of AchE activity, measured by the method of Ellman et al. (*26*), was 9.4 (data not shown). This occurred because striatal AchE activity is so high that [^{14}C]MP4P uptake reached saturation and was no longer dependent on AchE activity. The cortex/cerebellum ^{14}C uptake ratio (1.6), however, was close to that of AchE activity (1.8) (data not shown), suggesting that at the level of AchE activity in the cortex and cerebellum, [^{14}C]MP4P can respond well to changes in AchE activity. When the blood flow difference between the cortex and cerebellum was taken into account (cortex/cerebellum [^{123}I]IMP uptake ratio 1.5, data not shown), the reduction in [^{14}C]MP4P uptake under conditions of a 50% reduction in AchE activity was estimated to be 30%. This [^{14}C]MP4P response value obtained in the regional study is close to the R_{50} value observed in the NBM-lesion study (27%) (Table 3), suggesting that regional uptake of [^{14}C]MP4P can also be explained by the same model (Appendix, Equation A1).

CONCLUSION

We examined the sensitivities of three radioactive acetylcholine analogs (N[^{14}C]methyl-4-piperidyl esters) in rats with a unilateral NBM lesion. We demonstrated that both [^{14}C]MP4A and [^{14}C]MP4P had sufficient sensitivity to detect a reduction in cortical AchE activity of less than 50%, the putative change corresponding to the early stages of Alzheimer's disease. We also found that the sensitivity of the tracer was dependent on both its specificity for and reactivity with AchE in the brain region of interest. Therefore, to apply the present method to PET studies in humans, we need to assess whether the specificity for AchE and the reactivity of these tracers in the human brain are adequate. In our preliminary studies using postmortem human brain tissues, both [^{14}C]MP4A and [^{11}C]MP4P showed high cortical AchE specificity (94% and 86%, respectively) and adequate reactivity (details will be presented elsewhere). On the basis of these findings, we believe that [^{11}C]MP4A and [^{11}C]MP4P will be sensitive enough to detect a reduction in AchE activity in the human cortex of less than 50% and will be useful for the early and differential diagnosis of Alzheimer's disease. PET studies with [^{11}C]MP4A and [^{11}C]MP4P in humans and monkeys are currently in progress.

APPENDIX

Three-Compartmental Model for Kinetic Behavior of Carbon-14 Methyl-4-piperidyl Esters in Rat Brain

From the model shown in Figure 4, the amount of radioactive metabolite (M) remaining in a brain region during the stationary phase is given as follows:

$$M = RF \cdot K_1 \cdot AUC \cdot \exp(-k_4 \cdot T); \qquad RF = \frac{k_3}{k_2 + k_3}, \quad \text{Eq. A1}$$

where K_1, K_2, k_3 and k_4 are the transfer rate constants between compartments; AUC is the area under the plasma concentration–time curve of the lipophilic ester; and T is the observation time. The right side of Equation A1 consists of the following three parts: the retention fraction (RF) of the tracer $k_3/(k_2 + k_3)$; the cumulative input $K_1 \cdot AUC$; and the exponential term $\exp(-k_4 \cdot T)$, which represents the slow elimination of the hydrophilic metabolite (M) from the brain. Using the relationships $k_2 = FE/\lambda$ and $k_3 = k_{AchE}[AchE] + k_{Others}[Others]$, RF becomes

$$RF = \frac{k_{AchE}[AchE] + k_{Others}[Others]}{FE/\lambda + k_{AchE}[AchE] + k_{Others}[Others]}, \quad \text{Eq. A2}$$

where F is blood flow, E the extraction efficiency and λ the partition coefficient of the tracer between the brain and blood. Note that RF is a nonlinear function of the tracer's metabolic rate $k_{AchE}[AchE] + k_{Others}[Others]$. Equation A2 describes the basic relationships between tracer response and tracer parameters or between tracer response and in vivo parameters. Equation A2 is subsequently used to calculate the theoretical tracer response to the AchE activity change in NBM-lesioned rats. Furthermore, it provides a basis for tracer selection for human PET studies by extrapolating animal data to humans (see Conclusion).

Calculation of Theoretical Tracer Uptake Change Value at 50% AchE Activity Reduction Based on Three-Compartmental Model

To establish the relationship between tracer structure and tracer sensitivity for detecting cortical AchE activity changes in the NBM-lesioned rat model system, we calculated theoretical values of ^{14}C uptake changes at 50% AchE activity reduction (R_{50}), which is defined by

$$R_{50} = \frac{M(c) - M(l)}{M(c)} \times 100\%, \quad \text{Eq. A3}$$

where M(l) and M(c) represent ^{14}C uptake in the lesioned (l) and control (c) sides, respectively. Note that in Equation A1, the term $K_1 \cdot AUC \cdot \exp(-k_4 \cdot T)$ is the same for the lesioned and control

sides because F was the same in both sides, and k_4 is a constant parameter. In this case, M(l)/M(c) = RF(l)/RF(c). Then,

$$R_{50} = \left(1 - \frac{M(l)}{M(c)}\right) \times 100\% = \left(1 - \frac{RF(l)}{RF(c)}\right) \times 100\%. \quad \text{Eq. A4}$$

Thus, theoretical R_{50} values for the three N[^{14}C]methyl-4-piperidyl esters can be calculated if RF(l) and RF(c) are known. Under the conditions of 50% AchE activity reduction in the lesioned side compared with the control side, RF(l) and RF(c) are given as follows:

$$RF(l) = \frac{0.5 \times k_{AchE}[AchE] + k_{Others}[Others]}{FE/\lambda + 0.5 \times k_{AchE}[AchE] + k_{Others}[Others]},$$

for the lesioned side;

Eq. A5

$$RF(c) = \frac{k_{AchE}[AchE] + k_{Others}[Others]}{FE/\lambda + k_{AchE}[AchE] + k_{Others}[Others]},$$

for the control side.

In calculating RF(l), RF(c) and the calculated R_{50} values presented in Table 3, the following values were used for each parameter on the right side of Equation A5: k_{AchE}[AchE] and k_{Others}[Others] = the measured in vitro hydrolysis rates of the tracer by AchE and by other enzymes, respectively (Table 1); F (rat cortical blood flow) = 1.4 ml/g tissue/min (our unpublished data); E (extraction efficiency of tracer by brain) = 1; and λ (brain/blood partition coefficient) = 0.8 (it is known that λ = 0.7–0.9 for most lipophilic compounds).

ACKNOWLEDGMENTS

This work was supported in part by special coordination funds for the promotion of science and technology of the National Institute of Radiological Sciences and a Grant-in-Aid for Scientific Research (B), No. 05454197, from the Japanese Ministry of Education.

REFERENCES

1. Pope A, Hess HH, Lewin E. Microchemical pathology of the cerebral cortex in presenile dementia. *Trans Am Neurol Assoc* 1965;89:15–16.
2. Davies P, Maloney AFJ. Selective loss of central cholinergic neurons in Alzheimer's disease. *Lancet* 1976;2:1403.
3. Perry EK, Tomlinson BE, Blessed G, Bergmann K, Gibson PH, Perry RH. Correlation of cholinergic abnormalities with senile plaques and mental test scores in senile dementia. *BMJ* 1978;2:1457–1459.
4. Terry RD, Davies P. Dementia of the Alzheimer type. *Ann Rev Neurosci* 1980;3:77–95.
5. Gottfries CG. Alzheimer's disease and senile dementia: biochemical characteristics and aspects of treatment. *Psychopharmacology* 1985;86:245–3252.
6. Wyper DJ, Brown D, Patterson J, et al. Deficits in iodine-labeled 3-quinuclidinyl benzilate binding in relation to cerebral blood flow in patients with Alzheimer's disease. *Eur J Nucl Med* 1993;20:379–386.
7. Eckelman WC, Reba RC, Rzeszotarski WJ, et al. External imaging of cerebral muscarinic acetylcholine receptors. *Science* 1984;223:291–293.
8. Mulholland GK, Jung Y-W, Wieland DM, Kilbourn MR, Kuhl DE. Synthesis of [^{18}F]fluoroethoxybenzovesamicol, a radiotracer for cholinergic neurons. *J Labd Compd Radiopharm* 1993;33:583–592.
9. Dannals RF, Langstrom B, Ravert HT, Wilson AA, Wagner HN Jr. Synthesis of radiotracers for studying muscarinic cholinergic receptors in the living human brain using positron emission tomography: [^{11}C]dexetimide and [^{11}C]levetimide. *Appl Radiat Isot* 1988;39:291–295.
10. Dewey SL, MacGregor R, Brodie JD, et al. Mapping muscarinic receptors in human and baboon brain using [N-^{11}C-methyl]-benztropine. *Synapse* 1990;5:213–223.
11. Vora MM, Finn RD, Booth TE. [N-methyl-^{11}C]Scopolamine: synthesis and distribution in the rat brain. *J Labd Compd Radiopharm* 1983;20:373–379.
12. Jung Y-W, Van Dort ME, Gildersleeve DL, Wieland DM. A radiotracer for mapping cholinergic neurons of the brain. *J Med Chem* 1990;33:2065–2068.
13. Kuhl DE, Koeppe RA, Fessler JA, et al. In vivo mapping of cholinergic neurons in the human brain using SPECT and IBVM. *J Nucl Med* 1994;35:405–410.
14. Efange SMN, Dutta AK, Michelson RH, et al. Radioiodinated 2-hydroxy-3-(4-iodophenyl)-1-(4-phenylpiperidinyl)propane: potential radiotracer for mapping central cholinergic innervation in vivo. *Nucl Med Biol* 1992;19:337–348.
15. Widen L, Eriksson L, Ingvar M, Parsons SM, Rogers GA, Stone-Elander S. Positron emission tomographic studies of central cholinergic nerve terminals. *Neurosci Lett* 1992;136:1–4.
16. Prenant C, Crouzel C. Synthesis of [^{11}C]-sarin. *J Labd Compd Radiopharm* 1990;28:645–651.
17. Bonnot-Lours S, Crouzel C, Prenant C, Hinnen F. Carbon-11-labeling an inhibitor of acetylcholinesterase: [^{11}C]physostigmine. *J Labd Compd Radiopharm* 1993;33:277–284.
18. Tavitian B, Pappata S, Planas AM, et al. In vivo visualization of acetylcholinesterase with positron emission tomography. *Neuroreport* 1993;4:535–538.
19. Mulholland GK, Sugimoto H, Jewett DM, Kilbourn MR. Simple preparation of a novel C-11 acetylcholinesterase inhibitor [Abstract]. *J Nucl Med* 1989;30:822.
20. Irie T, Fukushi K, Iyo M. Evaluation of phenylmethanesulfonyl fluoride (PMSF) as a tracer candidate mapping acetylcholinesterase (AchE) in vivo. *Nucl Med Biol* 1993;20:991–992.
21. Irie T, Fukushi K, Akimoto Y, Tamagami H, Nozaki T. Design and evaluation of radioactive acetylcholine analogs for mapping brain acetylcholinesterase (AchE) in vivo. *Nucl Med Biol* 1994;21:801–808.
22. Namba H, Irie T, Fukushi K, Iyo M. In vivo measurement of acetylcholinesterase activity in the brain with a radioactive acetylcholine analog. *Brain Res* 1994;667:278–282.
23. Bayliss BJ, Todrik A. The use of selective acetylcholinesterase inhibitor in estimation of pseudocholinesterase activity in rat brain. *Biochem J* 1956;62:62–67.
24. Augustinsson KB. Assay methods for cholinesterase. In: Glick D, eds. *Methods of biochemical analysis*, vol. 5. New York: Wiley (Interscience); 1957:1–64.
25. Lear JL, Ackerman RF, Kameyama M, Kuhl DE. Evaluation of [^{123}I]isopropyliodoamphetamine as a tracer for local cerebral blood flow using direct autoradiographic comparison. *J Cereb Blood Flow Metab* 1982;2:179–185.
26. Ellman GL, Courtney KD, Andres V Jr, Featherstone RM. A new and rapid colorimetric determination of acetylcholinesterase activity. *Biochem Pharmacol* 1961;7:88–95.
27. Namba H, Irie T, Fukushi K, Yamasaki T, Tateno Y, Hasegawa S. Lesion of the nucleus basalis magnocellularis does not affect cerebral cortical blood flow in rats. *Neurosci Res* 1991;12:463–467.
28. Koelle GB, Friedenwald JS. A histochemical method for localizing cholinesterase activity. *Proc Soc Exp Biol Med* 1949;70:617–622.
29. Smith G. Animal models of Alzheimer's disease: experimental cholinergic denervation. *Brain Res Rev* 1988;13:103–118.
30. Johnston MV, McKinney M, Coyle JT. Neocortical cholinergic innervation: a description of extrinsic and intrinsic components in the rat. *Exp Brain Res* 1981;43:159–172.
31. Nagel JS, Scheiner SJ, Holman BL, Gibson RE, Wurzman RJ. Ibotenic lesioning of the nucleus basalis in the rat—a model of the cholinergic lesion seen in Alzheimer's disease [Abstract]. *J Nucl Med* 1986;27:913.
32. Kilbourn MR. Shades of gray: radiopharmaceutical chemistry in the 1990s and beyond. *Nucl Med Biol* 1992;19:603–606.
33. Lassen NA, Andersen AR, Friberg L, Paulson OB. The retention of [^{99m}Tc]-d,l-HMPAO in the human brain after intracarotid bolus injection: a kinetic analysis. *J Cereb Blood Flow Metab* 1988;8:S13–S22.